Pressure measurement based on multi-waves fusion algorithm

Hongliang Zhou[1]*,Hanhua Zhou[1], Hongjian Zhang[1], Xiaocheng Ge[2], Yanjie Zhao[1] and Weibin Lin[1]

[1] State Key Laboratory of Industrial Control Technology, College of Control Science and Engineering, Zhejiang University, Hangzhou, 310027, China
[2] School of Computing and Engineering, University of Huddersfield, UK
* zjuzhl@zju.edu.cn

Abstract: Measuring the pressure of a pressure vessel accurately is one of fundamental requirements of the operation of many complex engineering systems. Ultrasonic technique has been proposed to be a good alteration of non-intrusive measurement. Based on the study of acoustoelastic effect and thin-shell theory, it has been identified that the travel-time changes of the critically refracted longitudinal wave (L_{CR} wave) and other reflected longitudinal waves are all proportional to the inner pressure. Considering the information redundancy in these waves, we proposed an approach for pressure measurement by using the information fusion algorithm on multiple reflected longitudinal waves. In the paper, we discussed the fusion algorithm in details and proposed a pressure measurement model, which represents an accurate relationship between the pressure and the travel-time changes of multiple waves. Through the experiment, the analysis of data collected from experiment system showed that the pressure measurement based on the multi-wave model is notably more accurate than the one based on the single-wave model (the average relative error (ARE) can be less than 7.24% and the root-mean-square error (RMSE) can be lower than 0.3MPa).

Keywords: Pressure measurement, non-intrusive, the critically refracted longitudinal wave, reflected longitudinal waves, multiple waves, data fusion

1. Introduction

Pressure vessel is one of most commonly used components in many complex engineering systems. It is one of fundamental requirements to be able to accurately measure the inner pressure of a closed container so that we can adequately monitor and control the system's operating environment. Furthermore, we often need to deduct other important information from the pressure measurement, e.g. leakage. Traditionally, the pressure can be measured via intrusive method, i.e. drilling holes on the vessel's wall and mounting the measuring instrument inside. This method can provide a certain level of accuracy in the measurement. However it will usually change the structural integrity of the vessel, and also often increase the difficulty and cost of the vessel's maintenance. In some circumstance, a non-intrusive method is more attractive. So far, there are many approaches of non-intrusive measurement have been proposed, for example, the strain gauge method [1] and capacitor method [2]. All these non-intrusive measurement methods can solve some problems, but there is always a space for the improvement, in terms of applicability, accuracy, and lower cost etc.

Ultrasonic technique, as a nondestructive testing method, has been widely adopted in the stress measurement [3-6] and defect detection [7-10]. In the field of pressure measurement, Guers et al. [11]

have established the relationship between the amplitude of reflected ultrasonic wave and the pressure, and measured the pressure by computing the reflected ultrasonic signals from the fluid-vessel interface. Zhang et al. [12, 13] have analyzed the acoustoelastic effect in the thin-walled vessels and proposed a method of pressure measurement based on the observation that the propagation velocity of the ultrasonic wave is usually influenced by the stress on the vessel wall. In our previous research [14], we identified that the surface wave and the critically refracted longitudinal wave (L_{CR} wave) are all susceptible to the roughness of the vessel's outer surface. Instead of measuring L_{CR} wave, we concluded that the signal-to-noise ratio (SNR) and the sensitivity in the measurement can be significantly improved by taking the reflected longitudinal waves into the measurement. However, it has been widely discussed, e.g., in [6, 15, 16], that some environmental factors, mainly the temperature, can significantly influence the acoustoelastic effect of the ultrasonic waves, which will result in low accuracy in pressure measurement.

The ultimate goal of our research is to improve the accuracy of the ultrasonic measurement approach. In order to improve the measurement accuracy, we concluded in previous research that it is necessary to be able to detect the surface wave, L_{CR} wave and the reflected longitudinal waves so that the time that all these waves travel from the transmitter to the receiver can be measured, then the travel-time changes caused by the pressure can be computed. However, the changes of travel-time are too small to be measured precisely due to the receiver's sensitivity. In order to solve the problem, we proposed a new pressure measurement model based on the information fusion of measuring multiple waves, including the L_{CR} wave and the reflected longitudinal waves. The measurement model reflects the relationship between the pressure and the travel-time change of these multiple waves. Through the experiment, we were able to demonstrate that our model can effectively improve the measurement accuracy without the need to measure the temperature.

2. Generation of the multiple waves in the vessel wall

As shown in Fig. 1, when the longitudinal wave is incident from the polymethyl methacrylate (PMMA) wedge to the outer wall of pressure vessel with the first critical angle (α), waveform transformation will happen at the interface. The refracted longitudinal wave and refracted shear wave will be generated. Based on the Snell's Law(as described in Eq.(1)) [17]，the refracted angle of the refracted longitudinal wave was 90°.

$$\frac{\sin\alpha}{v_1} = \frac{\sin\gamma}{v_2} = \frac{\sin\beta}{v_3} \tag{1}$$

Where v_1, v_2 is the velocity of longitudinal wave in PMMA wedge and in the vessel wall, respectively. v_3 is the velocity of shear wave in the vessel wall. α, γ is the incident angle and refracted angle of longitudinal wave, respectively. And β, is the refracted angle of refracted shear wave.

The generated longitudinal wave is called the critically refracted longitudinal wave (L_{CR} wave). L_{CR} wave has been widely adopted in the stress measurement [3-5]. The L_{CR} wave propagates along the outer wall and is received by the receiving probe. The penetration depth of L_{CR} wave is between 1.5 and 1.8 wavelengths[18]. So the surface roughness of the vessel wall affects the propagation of L_{CR} wave greatly. The refracted shear wave with the refracted angle (β) will reach the inner wall, where waveform transformation will happen again and generate the first inner reflected longitudinal wave (Lre-I1st) and the first reflected shear wave (Sre-1st), as shown in Fig. 1. According to the Snell's Law, Lre-I1st wave will travel along the inner wall with the reflected angle of 90° . The Sre-1st wave will continue to travel in the vessel wall and then reach the outer wall, where it will generate the first reflected longitudinal wave (Lre-1st) and the second reflected shear wave (Sre-2nd). Similar with the L_{CR} wave, Lre-1st wave will travel along the outer wall and reach the receiving probe. The Sre-2nd wave will continue to travel in the vessel wall and generate the second inner reflected longitudinal wave (Lre-I2nd) and the third reflected shear wave (Sre-3rd), and so on. Therefore, the receiving probe will successively receive multiple waves, including L_{CR} wave, Lre-1st wave, Lre-2nd wave and so on, as show in Fig. 2. The time interval Δt_i between the L_{CR} wave and the Lre-1st wave is definite, so is that between the neighboring reflected longitudinal waves. The time interval can be described as:

$$\Delta t_i = \frac{2d}{C_S \cos\beta} - \frac{2d \tan\beta}{C_L} \tag{2}$$

where d is the thickness of the vessel wall, β β is the refracted angle of the shear wave propagating inside the wall, C_S and C_L are the speeds of the shear wave and longitudinal wave in the pressure vessel, respectively.

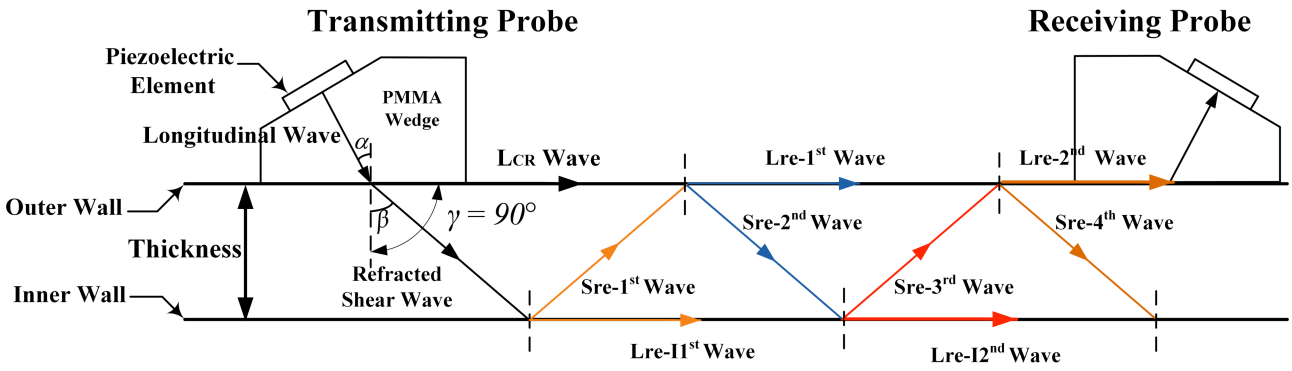

Fig. 1. *Propagation of multiple waves inside the vessel wall*

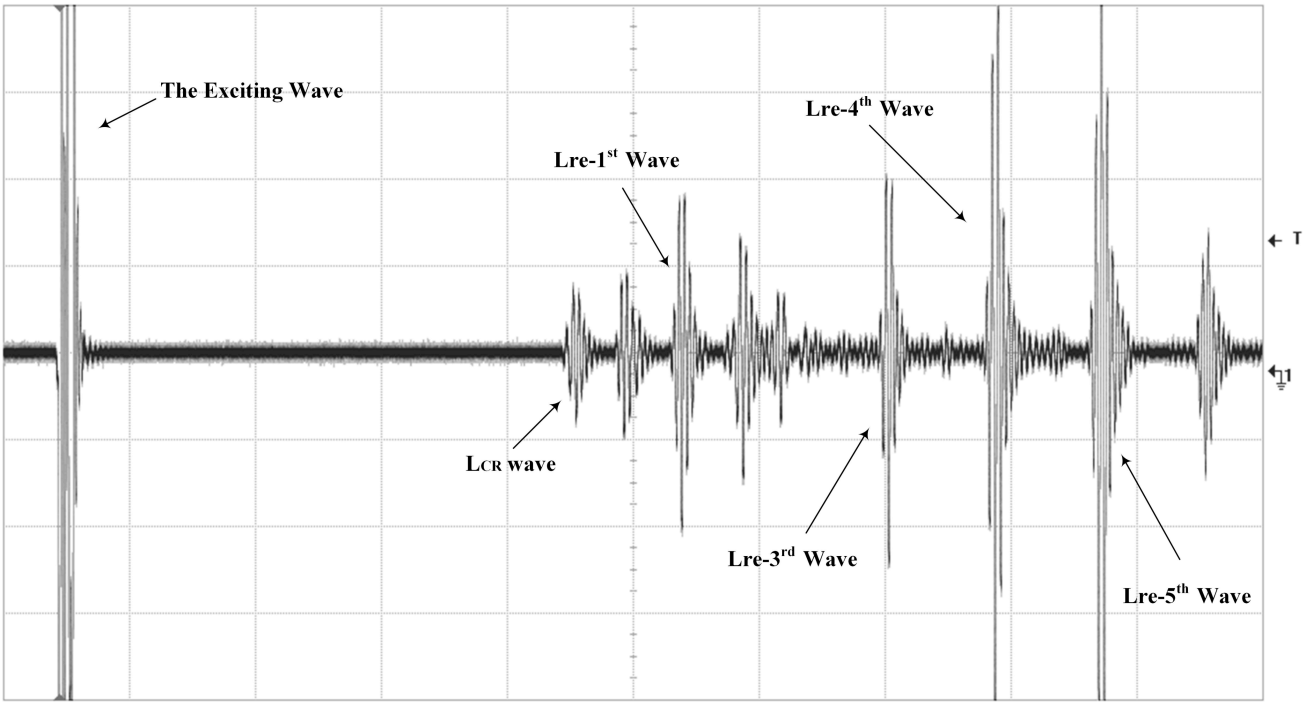

Fig. 2. *Ultrasonic signal received by the receiving probe*

3. Pressure measurement method based on ultrasonic waves

3.1. Relationship between the pressure and the travel-time change of L_{CR} wave

As developed by Hughes and Kelly [19], the relationship between the wave speeds and the strain in the pressure vessel obeys the following expressions:

$$\rho_0 V_{AA}^2 = \lambda + 2\mu + (2l + \lambda)(\varepsilon_A + \varepsilon_R + \varepsilon_C) + (4m + 4\lambda + 10\mu)\varepsilon_A \tag{3}$$

$$\rho_0 V_{AR}{}^2 = \mu + (m + \lambda)(\varepsilon_A + \varepsilon_R + \varepsilon_C) + 4\mu\varepsilon_A + 2\mu\varepsilon_R - \frac{1}{3}n\varepsilon_C \tag{4}$$

where V_{AA} V_{AA} is the longitudinal wave velocity along the axial direction of the pressure vessel wall. ε_A ε_A, ε_R ε_R and ε_C are the strains along the axial, radial and circumferential directions of the vessel wall, respectively. ρ_0 is the initial density of the pressure vessel. λ and μ are the second-order elastic constants, while l, m, and n are the third-order elastic constants.

According to the Hooke's Law, relationships between the strain components in three orthogonal directions and stress can be derived as:

$$\varepsilon_A = \frac{1}{E}(\sigma_A - \nu\sigma_C) \tag{5}$$

$$\varepsilon_R = -\frac{\nu}{E}(\sigma_A + \sigma_C) \tag{6}$$

$$\varepsilon_C = \frac{1}{E}(\sigma_C - \nu\sigma_A) \tag{7}$$

where E is the elasticity modulus of vessel material, υ is the Poisson's ratio, σ_A and σ_C are the axial stress and the circumferential stress, respectively.

Based on the thin-shell theory [20], the stress field in the vessel wall is two-dimensional, including the stress in the axial direction and that in the circumferential direction, as described by:

$$\sigma_A = \frac{pR}{2d} \tag{8}$$

$$\sigma_C = \frac{pR}{d} \tag{9}$$

where p is internal pressure of the vessel, R is the average radius of the vessel, and d is the thickness of the vessel wall.

Besides, the speed of the longitudinal wave can also be described by:

$$V_L^0 = \frac{D}{t_L^0} \tag{10}$$

$$V_L = \frac{D}{t_L} \tag{11}$$

where t_L^0 (V_L^0) and t_L (V_L) are the travel-time (speed) of the longitudinal wave under the free pressure state and measured pressure state, respectively. D is the propagation distance of the longitudinal wave.

With the Eqs.(3)-(11), the relationship between the pressure and the travel-time change of longitudinal wave can be derived as:

$$p = -\frac{E}{L_1}\frac{d}{R}\frac{\Delta t_L}{t_L^0} \tag{12}$$

where p is the pressure change, Δt_L is the travel-time changes of the longitudinal wave ($\Delta t_L = t_L - t_L^0$), and L_1 is the acoustoelastic constant for the longitudinal wave, as given by:

$$L_1 = \frac{1}{4}\frac{6l + 7\lambda + 4m + 10\mu - 12l\nu - 14\lambda\nu - 8m\nu - 20\mu\nu}{\lambda + 2\mu} \tag{13}$$

The L_{CR} wave is a special longitudinal wave that propagates along the outer wall, so Eq. (13) is also applicable for the L_{CR} wave. Obviously, the travel-time change of L_{CR} wave is proportional to the pressure change.

3.2. Relationship between the pressure and the travel-time change of reflected longitudinal waves

As analyzed in Sec. 2, the reflected longitudinal wave along the outer wall is generated by the reflected shear wall in the wall. So it is necessary to obtain the model between the pressure and the travel-time change of reflected shear wave. Like the longitudinal wave, the model can be developed by:

$$p = -\frac{E}{L_2}\frac{d}{R}\frac{\Delta t_{Sre}}{t^0_{Sre}} \tag{14}$$

where t^0_{Sre} (t_{Sre}) is the travel-time of the reflected shear wave under the free pressure state (the measured pressure state)， Δt_{Sre} is the travel-time change for the reflected shear wave ($\Delta t_{Sre} = t_{Sre} - t^0_{Sre}$). L_2 is the acoustoelastic constant for the reflected shear wave, as given by:

$$L_2 = \frac{1}{12}\frac{9\lambda + 9m - 18\lambda\nu - 18m\nu - 45\mu\nu + m\nu + 9\mu - 2n - 3\mu(1+\nu)\cos 2\beta}{\mu} \tag{15}$$

The travel-time change of the reflected longitudinal wave (Δt_{Lre}) consists of two parts. One part is the travel-time change of the shear wave reflected inside the vessel wall. The other is the travel-time change of the longitudinal wave propagating along the outer wall. Therefore, Δt_{Lre} can be given by:

$$\Delta t_{Lre} = \Delta t_{Sre} + \Delta t_L = -\frac{p}{E}\frac{R}{d}(L_1 t^0_L + L_2 t^0_{Sre}) \tag{16}$$

Eq.(16) shows that, like the L_{CR} wave, the travel-time change of the reflected longitudinal wave is proportional to the pressure change, too.

3.3. Pressure measurement model with temperature compensation based on a single wave

Temperature is an important factor for ultrasonic measurement technique [6, 15, 16]. Some parameters in Eq. (12) and Eq. (16), such as L_1 and L_2, are affected by the temperature. In practical application, the relationship between the pressure and the travel-time change of L_{CR} wave (the reflected longitudinal waves) can be described by [21]:

$$\Delta t^{(p,\Delta T)}_{L_{CR}} = K_{p0}p + K_{T0}\Delta T \tag{17}$$

$$\Delta t^{(p,\Delta T)}_{Lre-n^{th}} = K_{pn}p + K_{Tn}\Delta T \tag{18}$$

where $\Delta t^{(p,\Delta T)}_{L_{CR}}$ ($\Delta t^{(p,\Delta T)}_{Lre-n^{th}}$) is the measured travel-time change of L_{CR} wave (the nth reflected longitudinal wave), K_{p0} (K_{pn}) is the pressure coefficient of L_{CR} wave (the nth reflected longitudinal wave), K_{T0} (K_{Tn})

is the temperature coefficient of L_{CR} wave (the nth reflected longitudinal wave). ΔT is the temperature change ($\Delta T = T - T_0$). T and T_0 are the measured temperature and the reference temperature, respectively.

With Eq.(17)-(18), the pressure measurement model based on a single wave (L_{CR} wave or the reflected longitudinal wave) with temperature compensation can be derived as:

$$p = \frac{1}{K_{p0}} \Delta t_{L_{CR}}^{(p,\Delta T)} - \frac{K_{T0}}{K_{p0}} \Delta T \tag{19}$$

$$p = \frac{1}{K_{pn}} \Delta t_{Lre-n^{th}}^{(p,\Delta T)} - \frac{K_{Tn}}{K_{pn}} \Delta T \tag{20}$$

With Eq. (19) or Eq. (20), the pressure measurement can be implemented by measuring the travel-time change and the temperature change. However, the pressure measurement accuracy is overly dependent on the accuracy of travel-time and the stability of the temperature. Hence, it is very difficult to achieve high measuring accuracy.

3.4. Pressure measurement method based on multi-waves fusion algorithm

Eq. (17)-(18) shows that both the travel-time change of the L_{CR} wave and reflected longitudinal waves change linearly with the pressure and temperature. Considering the information redundancy among those waves, it is possible to improve the measuring accuracy by the fusion algorithm. Therefore, a new method based on multiple waves is proposed, as described by:

$$p = A_0 \Delta t_{L_{CR}}^{(p,\Delta T)} + \sum_{n}^{N} A_n \Delta t_{Lre-n^{th}}^{(p,\Delta T)} + B\Delta T \tag{21}$$

where N is the total number of the receiving reflected longitudinal waves, which is determined by the distance between the transmitting probe and receiving probe. A_0 (A_n) is the travel-time coefficient of L_{CR} wave (the nth reflected longitudinal wave), and B is the temperature coefficient.

With Eq. (21), it is obvious that the pressure measurement accuracy does not merely depend on the travel-time change of a single wave. Even though the travel-time change of someone has a certain error, it will not affect the measurement accuracy seriously. Therefore, Eq. (13) can improve the measureing accuracy to some extent. However it is still affected by the temperature change. Actually, according to Eq.(17)-(18), the travel-time change of each wave contains the information of temperature change. So the pressure measurement model can be developed by:

$$p = A_0 \Delta t_{L_{CR}}^{(p,\Delta T)} + \sum_{n}^{N} A_n \Delta t_{Lre-n^{th}}^{(p,\Delta T)} \tag{22}$$

In the following sections, experiments will be carried out to test the performance of the pressure measurement model described in Eq. (22).

4. Experiment system

As shown in Fig. 3, the experiment system consists of seven parts: pressure test pump, pressure vessel, biochemical incubator, ultrasonic probes, ultrasonic exciting circuit, high-speed acquisition system

and computer. In order to reduce the influence of temperature, the dual-receivers mode was adopted[14], which means three probes are arranged in the axial direction of the vessel, including one transmitter (T) and two receivers (R1, R2).

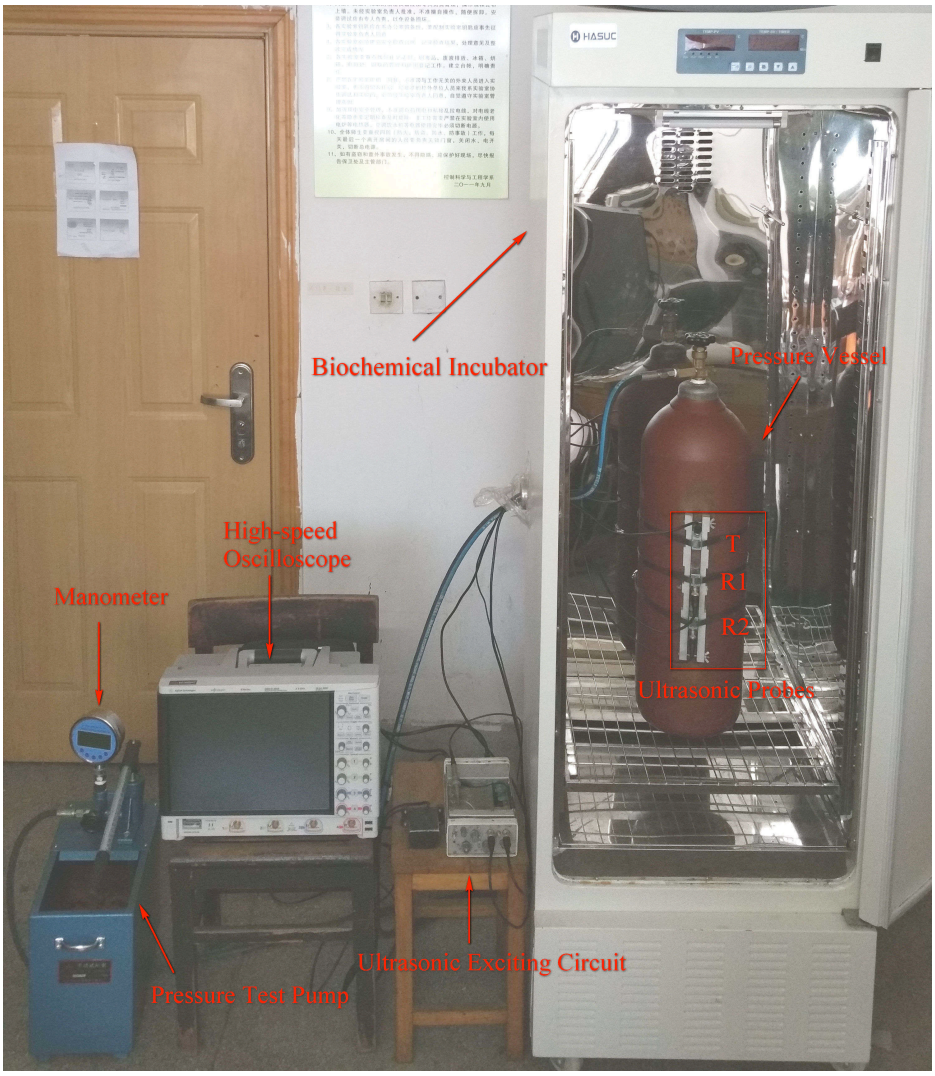

Fig. 3. *Experiment system*

The pressure test pump is utilized to change the internal pressure, which can be measured by the manometer with the full scale of 16 MPa and the maximum fiducial error of 0.4%. The ultrasonic signal is excited by the ultrasonic exciting circuit and received by the high-speed acquisition system with the sample rate of 20 GHz. The biochemical incubator is used to control the environment temperature. Besides, a computer is used to obtain the travel time between R1 and R2 by correlation algorithm.

In order to validate the feasibility of the method, two pressure vessels with different materials are tested, labeled as pressure vessel-I (PV-I) and pressure vessel-II (PV-II). The experiment parameters are

shown in Table 1, where the T-R1 is the distance between the probe T and R1, and so on. To avoid the stress concentration and boundary effect, the probes are arranged in the central area of the pressure vessel.

Table 1 Experiment parameters

Pressure Vessel No.	PV-I	PV-II
Component	37Mn	30CrMo
Outer Radius (mm)	109.5	114.5
Inner Radius (mm)	103.8	108.2
Thickness(mm)	5.7	6.3
Height(mm)	725	1110
T-R1(mm)	75	91
T-R2(mm)	138	138
R1-R2(mm)	63	47

5. Experiment results and discussion

5.1. Selection of the object waves

In the dual-receivers mode, both the probe R1 and R2 will receive a series of waves. Selecting waves that have a high SNR as object waves is beneficial to improve measuring accuracy of the travel-time between R1 and R2. Fig. 4 shows the multiple waves received by R1 and R2 in PV-I. For the dual-receivers mode, the accuracy of travel-time based on correlation algorithm depends on the quality of waves in both R1 and R2. Therefore, in this work, the L_{CR} wave, Lre-1^{st} wave, Lre-4^{th} wave and Lre-5^{th} wave are chosen as the object waves to measure the pressure in PV-I. And similarly in the PV-II, the object waves include the L_{CR} wave, Lre-4^{th} wave, Lre-5^{th} wave and Lre-6^{th} wave.

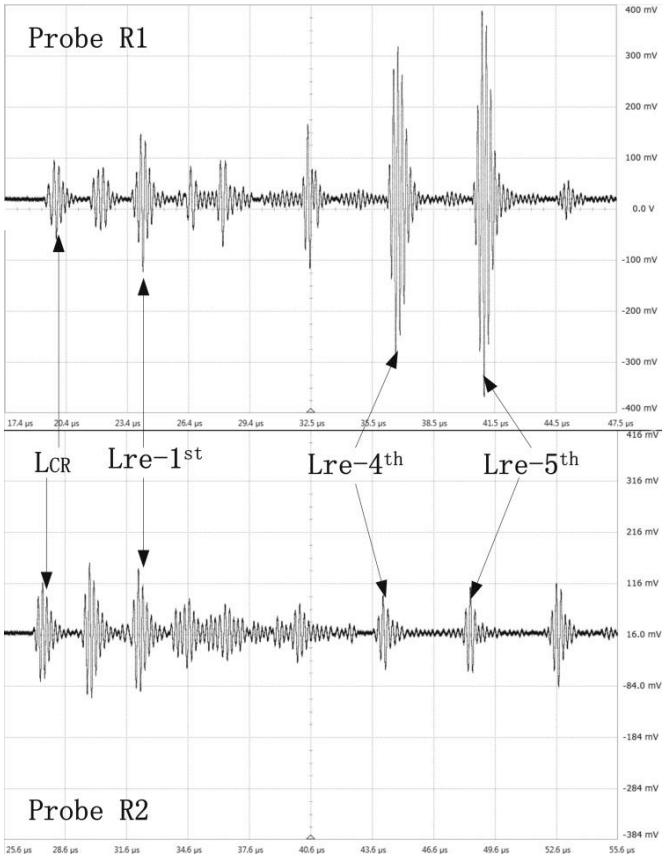

Fig. 4. *Multiple waves received by probe R1 and R2 in PV-I*

5.2. Travel-time change with temperature and pressure

Fig. 5 shows the travel-time changes ($\Delta t^{(\Delta T)}$) of multiple waves with temperature at zero pressure in PV-I and PV-II. The temperature in PV-I ranges from 18.0°C to 37.1°C, and that in PV-II ranges from 20.4°C to 38.3°C. The reference temperature, the reference travel-time of each wave and fitting results are shown in Table 2. The results show that the travel-time of each wave changes linearly with temperature in both pressure vessels, which is consistent with Eq.(17)-(18).

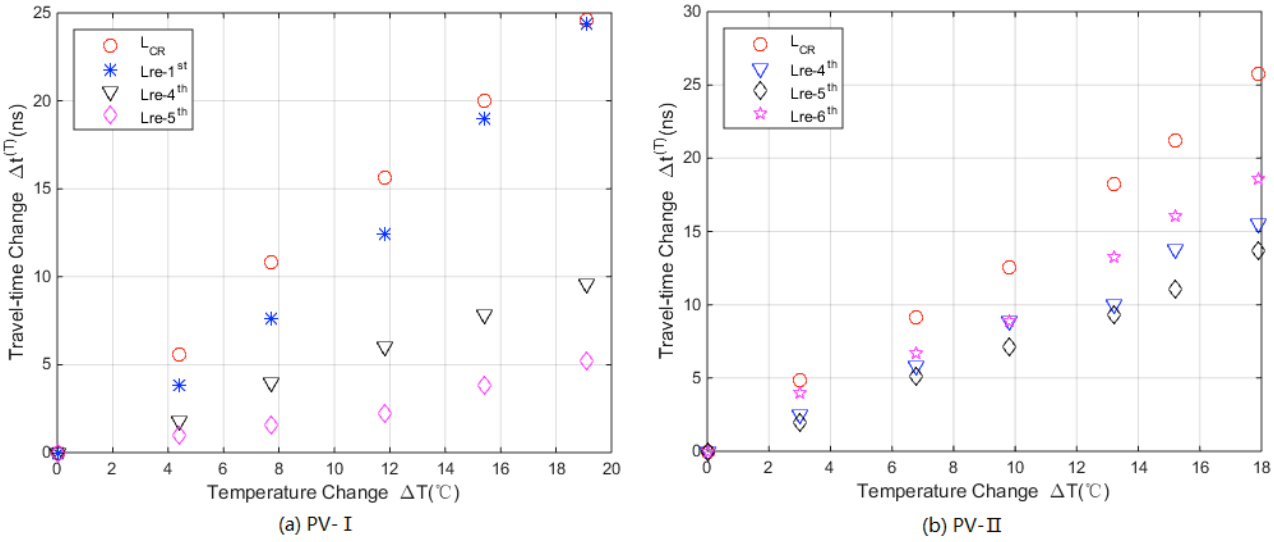

Fig. 5. *Travel-time changes of multiple waves with temperature at zero pressure*

Table 2 *Fitting results of the data points in Fig. 5*

Pressure vessel No.	PV-I				PV-II			
waves	L_{CR}	Lre-1st	Lre-4th	Lre-5th	L_{CR}	Lre-4th	Lre-5th	Lre-6th
Reference temperature (T_0) (℃)	18.0				20.4			
Reference travel-time (t0) (us)	10.691	10.734	10.480	10.592	7.673	7.543	7.567	7.713
Slope ($\Delta t^{(\Delta T)}$/ΔT) (ns/℃)	1.289	1.297	0.512	0.263	1.404	0.864	0.750	1.019
Correlation coefficient	0.998	0.984	0.998	0.961	0.995	0.988	0.997	0.991

The travel-time changes ($\Delta t^{(p,\Delta T)}$) of multiple waves with pressure are investigated at different temperatures in PV-I. The results are shown in Fig. 6. The results show that the travel-time of each wave increases nearly linearly with the pressure at a certain temperature, which is in good agreement with the models in Eq. (12) and Eq. (14). And the fitting results are shown in Table 3. It can be seen that the relationship between the travel-time change and the pressure remained appropriately invariable at different temperatures for each wave.

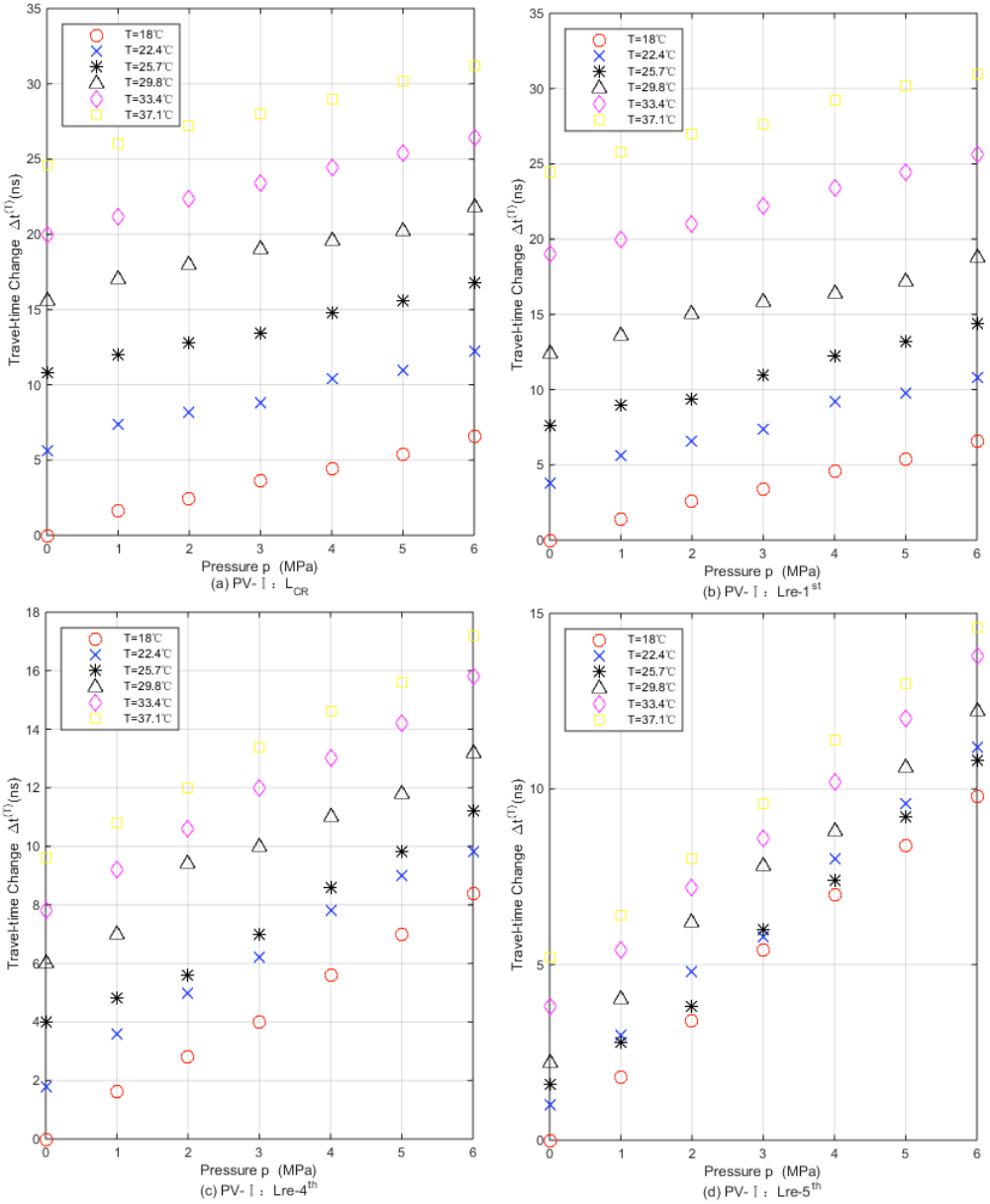

Fig. 6. *Travel-time changes of multiple waves with pressure at different temperatures in PV-I*

Table 3 *Fitting results of the data points in PV-I*

Waves	Slope at different temperatures Kp（ns/MPa）					
	18℃	22.4℃	25.7℃	29.8℃	33.4℃	37.1℃
L_{CR}	1.05	1.04	0.97	0.95	1.06	1.07
Lre-1st	1.06	1.14	1.13	0.99	1.11	1.10
Lre-4th	1.38	1.34	1.24	1.20	1.30	1.25
Lre-5th	1.65	1.68	1.57	1.64	1.65	1.60

Similar experiments are carried out in PV-II. The results are shown in Fig. 7. The temperature ranges from 20.4°C to 38.3°C. And the reference temperature and reference travel-time of multiple waves are shown in Table 2. The fitting results are shown in Table 4. After analysis, same conclusions can be obtained in PV-II.

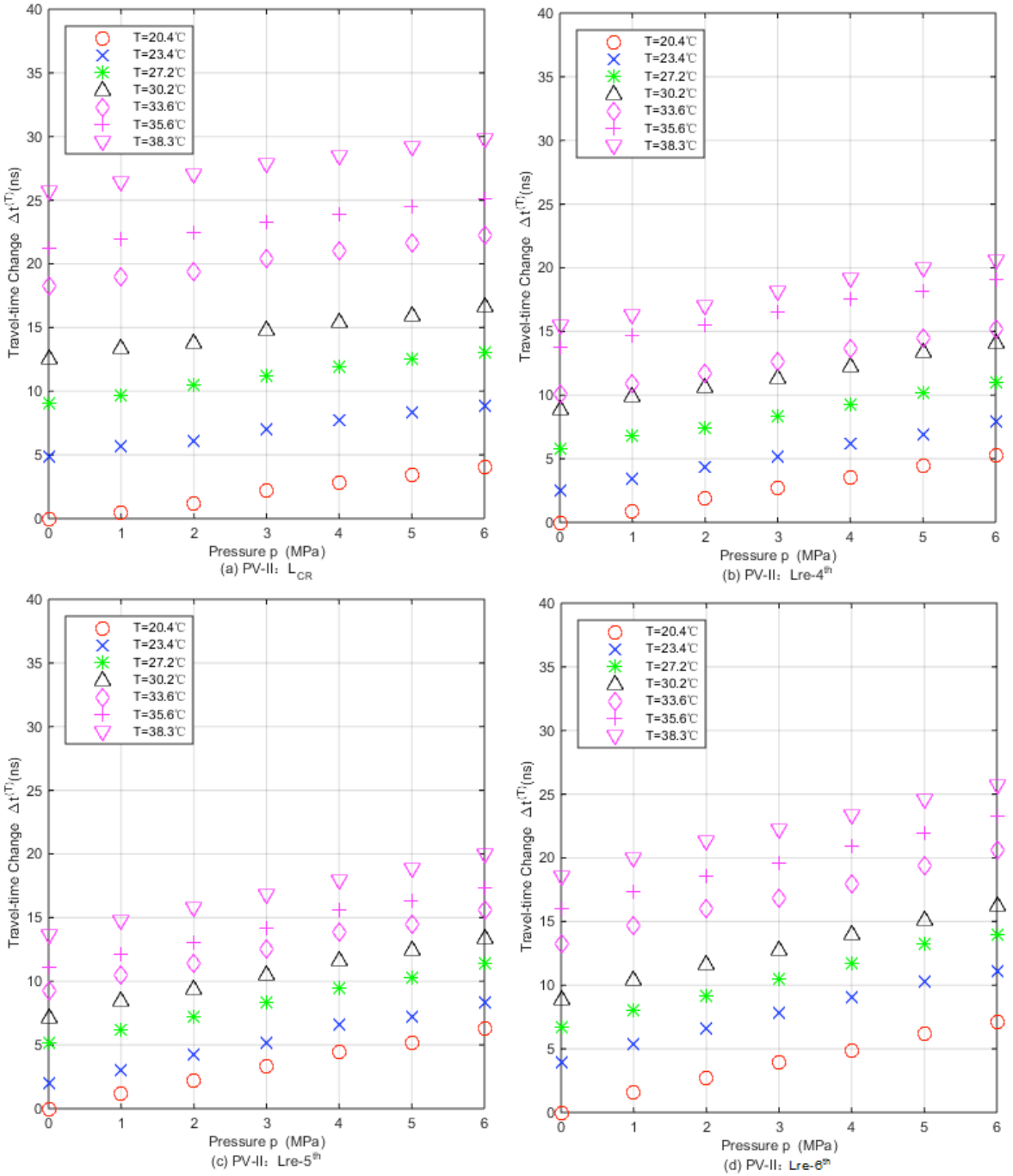

Fig. 7. *Travel-time changes of multiple waves with pressure at different temperatures in PV-II*

Table 4 Fitting results of the data points in *PV-II*

Waves	Slope at different temperatures Kp（ns/MPa）					
	20.4℃	23.4℃	27.2℃	30.2℃	33.6℃	35.6℃
L_{CR}	0.70	0.68	0.68	0.69	0.68	0.65
Lre-4th	0.88	0.90	0.86	0.87	0.88	0.88
Lre-5th	1.03	1.06	1.04	1.03	1.05	1.06
Lre-6th	1.16	1.20	1.24	1.20	1.20	1.19

5.3. Pressure measurement models based on different waves

To determine the coefficients in Eqs. (19)-(22), multiple linear regression analysis is employed in this work [22]. For the PV-I, the training data sets are shown in Fig.6. The possible pressure measurement models based on a single wave can be derived by:

$$p = 0.9617\Delta t_{L_{CR}}^{(p,\Delta T)} - 1.2377\Delta T - 0.3944 \tag{23}$$

$$p = 0.9016\Delta t_{L_{CR}}^{(p,\Delta T)} - 1.0664\Delta T - 0.1619 \tag{24}$$

$$p = 0.7654\Delta t_{L_{CR}}^{(p,\Delta T)} - 0.3749\Delta T - 0.0533 \tag{25}$$

$$p = 0.6017\Delta t_{L_{CR}}^{(p,\Delta T)} - 0.1460\Delta T - 0.0973 \tag{26}$$

where $\Delta t_{L_{CR}}^{(p,\Delta T)}$, $\Delta t_{Lre-1^{st}}^{(p,\Delta T)}$, $\Delta t_{Lre-4^{th}}^{(p,\Delta T)}$ and $\Delta t_{Lre-5^{th}}^{(p,\Delta T)}$ are the measured travel-time change of L_{CR} wave, Lre-1st wave, Lre-4th wave and Lre-5th wave in PV-I, respectively.

The pressure measurement models based on multiple waves and temperature change in PV-I is derived by:

$$p = 0.4494\Delta t_{L_{CR}}^{(p,\Delta T)} - 0.0535\Delta t_{Lre-1^{st}}^{(p,\Delta T)} + 0.0860\Delta t_{Lre-4^{th}}^{(p,\Delta T)} + 0.2965\Delta t_{Lre-5^{th}}^{(p,\Delta T)} - 0.6240\Delta T - 0.2416 \tag{27}$$

The final measurement models based on multiple waves in PV-I is derived by:

$$p = 0.0272\Delta t_{L_{CR}}^{(p,\Delta T)} - 0.1935\Delta t_{Lre-1^{st}}^{(p,\Delta T)} + 0.1334\Delta t_{Lre-4^{th}}^{(p,\Delta T)} + 0.6136\Delta t_{Lre-5^{th}}^{(p,\Delta T)} - 0.1813 \tag{28}$$

For the PV-II, the analysis data sets are shown in Fig. 7. The similar measurement model based on different waves can also be developed by multiple liner regression analysis, and the details are not given any more.

5.4. Experiment results for pressure measurement

In order to evaluate the performance of the different models described in Sec. 5.3, the average relative error (ARE), the root-mean-square error (*RMSE*) and correlation coefficient (*r*) are introduced, which can be described by:

$$\bar{X}=\frac{1}{n}\sum_{i=1}^{n}X_i \tag{29}$$

$$\mathrm{ARE}=\frac{1}{n}\sum_{i=1}^{n}\left|\frac{x_i'-x_i}{x_i}\right| \tag{30}$$

$$RMSE=\sqrt{\frac{1}{n}\sum_{i=1}^{n}(X_i-\bar{X})^2} \tag{31}$$

$$r=\frac{\sum_{i=1}^{n}(x_i'-\overline{x'})(x_i-\overline{x_i})}{\sqrt{\sum_{i=1}^{n}(x_i'-\overline{x'})^2\bullet\sum_{i=1}^{n}(x_i-\overline{x_i})^2}} \tag{32}$$

where x_i' (x_i) is the measured value (the true value) of the i-th time, $\overline{x'}$ ($\overline{x_i}$) is the average of the measured value (the true value), n is the number of measurement.

In the PV-I, the number of test data for each wave is 12 with the pressure ranged from 1.1MPa to 6MPa and the temperature ranged from18.9°C to 32.9°C. In the PV-II, the number of test data is 42 with the pressure ranged from 1MPa to 6MPa and the temperature ranged from16.2°C to 35.9°C. The test results are shown in Table. 5. The results validated the feasibility of the pressure measurement model based on multiple waves. Compared with the measurement model based on a single wave, which is easily affected by the temperature, the measurement model based on multiple waves can achieve the pressure measurement with the *ARE* less than 7.24% and the *RMSE* within 0.3MPa.

Table 5 Results of different pressure measurement models in PV-I and PV-II

Pressure vessel No.	PV-I			PV-II		
Measurement model based on different waves below	*ARE*	*RMSE* （MPa）	*r*	*ARE*	*RMSE* （MPa）	*r*
L_{CR}	43.01%	1.35	0.971	32.75%	1.17	0.831
Lre-1st	13.61%	0.57	0.925	------	-------	------
Lre-4th	15.38%	0.50	0.950	36.58%	1.03	0.869
Lre-5th	8.86%	0.39	0.981	47.78%	1.38	0.870
Lre-6th	-------	--------	-------	52.39%	1.67	0.779
Multiple waves+ΔT	15.74%	0.55	0.984	18.36%	0.79	0.938
Multiple waves	6.24%	0.26	0.987	7.24%	0.22	0.993

5.5. Discussion

The selection of object waves is critical to the accuracy of the pressure measurement model. In the dual-receivers mode, high SNR for object waves on both receiving probes are claimed in order to improve measuring accuracy of the travel-time change. This causes some uncertainty to the pressure measurement model based on multiple waves. in this work, the L_{CR} wave, Lre-1st wave, Lre-4th wave and Lre-5th wave are chosen as the object waves to establish the pressure measurement mode in PV-I. while in the PV-II, the object waves include the L_{CR} wave, Lre-4th wave, Lre-5th wave and Lre-6th wave.

The travel-time of the L_{CR} wave and the reflected longitudinal waves changes linearly with temperature and pressure. And the relationship between the travel-time change and the pressure remained appropriately invariable when the temperature changes in our study. This is the theoretical basis for the pressure measurement model with temperature compensation in Eqs. (23)-(26).

The experiment results show that the travel-time change induced by pressure is very small (1ns/MPa for L_{CR} wave) while the temperature's influence is very significant (1.3ns/℃ for L_{CR} wave). So how to

decrease the influence of the temperature and keep the temperature constant during the measuring process is critical. Pressure measurement model based on multiple waves take advantage of the information redundancy among the L_{CR} wave and the reflected longitudinal waves and can achieve higher accuracy than models based on single wave.

The training data and the test data are all results of individual measurement. Considering the measurement uncertainty, repeated measurement and averaging can improve the accuracy of the measurement further.

6. Conclusion

In this paper, we proposed a non-intrusive method for pressure measurement based on multiple waves. Both the theoretical analysis and experiment results show that the travel-time of L_{CR} wave and reflected longitudinal waves respectively changes linearly with the pressure and temperature. Considering the information redundancy among the travel-time change of these waves, the fusion algorithm is adopted to establish the pressure measurement model, which describes the relationship between the pressure and the travel-time changes of L_{CR} wave and that of reflected longitudinal waves.

With the dual-receivers mode, the measurement system is constructed to validate the feasibility and effectiveness of the new pressure measurement model. Compared with the pressure measurement model based on a single wave, the multi-wave model can effectively improve the measurement accuracy. Experiment shows that the new method can implement the pressure measurement with the *ARE* less than 7.24% and the *RMSE* within 0.3MPa. Furthermore there is no need to measure the temperature using this method, which can effectively minimize the temperature influence and simplify the measurement system.

Overall we can conclude from our research that:

(1) The travel-time change of L_{CR} wave and reflected longitudinal waves respectively varies linearly with the pressure and temperature.

(2) A multi-wave pressure measurement model with the fusion algorithm is proposed, which is able to adequately describe the relationship between the pressure and the travel-time changes of L_{CR} wave and that of reflected longitudinal waves.

(3) In the experiment we have demonstrated that the pressure measurement based on the multi-wave model is notably more accurate than the one based on the single-wave model (ARE is less than 7.24% and RMSE is lower than 0.3MPa).

(4) Last but not least, the multi-wave model can cancel the influence of the temperature. It can effectively minimize the temperature influence and simplify the measurement system. The travel-time change

induced by pressure is very small. Increasing the sample rate and using the averaged travel-time change of repeated measurement can improve the measurement accuracy further.

References:参考文献需要再次核对，包括正文引用

[1] K. Hoffmann, *An Introduction to Measurements Using Strain Gages: With 172 Figures and Tables*: Hottinger Baldwin Messtechnik GmbG, 1989.

[2] J. Huang, H. Yuan, Y. Cui, and Z. Zheng, "Nonintrusive pressure measurement with capacitance method based on FLANN," *Instrumentation and Measurement, IEEE Transactions on,* vol. 59, pp. 2914-2920, 2010.

[3] Y. Javadi, Y. Javadi and S. Hatef Mosteshary, "Evaluation of sub-surface residual stress by ultrasonic method and finite-element analysis of welding process in a monel pressure vessel," vol.45, pp. 2017.

[4] Y. Javadi and M. Ashoori, "Sub-surface stress measurement of cross welds in a dissimilar welded pressure vessel," *Materials & Design,* vol. 85, pp. 82-90, 2015-11-15 2015.

[5] Y. Javadi, M. Hasani and S. Sadeghi, "Investigation of Clamping Effect on the Welding Sub-surface Residual Stress and Deformation by Using the Ultrasonic Stress Measurement and Finite Element Method," *Journal of Nondestructive Evaluation,* vol. 34, pp. 1-11, 2015.

[6] D. Vangi and A. Virga, "A practical application of ultrasonic thermal stress monitoring in continuous welded rails," *Experimental Mechanics,* vol. 47, pp. 617-623, 2007.

[7] M. J. Guers and B. R. Tittmann, "In-situ ultrasonic measurements of creep specimens," *The Journal of the Acoustical Society of America,* vol. 139, pp. 2066-2066, 2016.

[8] M. Kesharaju, R. Nagarajah, T. Zhang, and I. Crouch, "Ultrasonic sensor based defect detection and characterisation of ceramics," *Ultrasonics,* vol. 54, pp. 312-317, 2014-01-01 2014.

[9] L. Le Jeune, S. Robert, E. L. Villaverde, and C. Prada, "Plane Wave Imaging for ultrasonic non-destructive testing: Generalization to multimodal imaging," *Ultrasonics,* vol. 64, pp. 128-138, 2016.

[10] J. L. Rose, J. J. Ditri, A. Pilarski, J. Zhang, F. Carr, and W. McNight, "A guided wave inspection technique for nuclear steam generator tubing," in *13th World Conference of Non-Destructive Testing*, 2012, pp. 191-195.

[11] M. J. Guers, C. J. Fontana, D. R. Zilinskis, and B. R. Tittmann, "Investigation of Noninvasive Approaches for Pressure Measurement," *Review of Progress in Quantitative Nondestructive Evaluation*, 2007, pp. 1653-1659.

[12] Z. Ling, H. Zhou and H. Zhang, "Nondestructive Pressure Measurement in Vessels Using Rayleigh Waves and L-CR Waves," *IEEE Transactions on Instrumentation and Measurement, ,* vol. 58, pp. 1578-1584, 2009.

[13] H. Zhang, Q. He and Y. Yan, "A new nondestructive technique for measuring pressure in vessels by surface waves," *Applied Acoustics,* vol. 69, pp. 891-900, 2008.

[14] Y. Bi, H. Zhou, Z. Huang, H. Zhou, and X. Yang, "Ultrasonic pressure measurement in pressure vessels," *Review of Scientific Instruments,* vol. 85, p. 125002, 2014.

[15] D. E. Bray, J. Vela and R. S. Al-Zubi, "Stress and temperature effects on ultrasonic properties in cross-linked and high density polyethylene," *Journal of pressure vessel technology,* vol. 127, pp. 220-225, 2005.

[16] K. Harkreader, "Effects of temperature on high density polyethylene piping and accuracy of ultrasonic thickness gaging," *Materials evaluation,* vol. 59, pp. 1033-1036, 2001.

[17] J. L. Rose, *Ultrasonic waves in solid media*: Cambridge university press, 2004.

[18] R. S. Fraga, M. H. Andrino and A. A. Santos, "Evaluation of the penetration depth of LCR waves for stress measurement," in *International Conference on Integrity, Reliability and Failure, Porto/Portugal July*, 2009.

[19] D. S. Hughes and J. L. Kelly, "Second-order elastic deformation of solids," *Physical review,* vol. 92, p. 1145, 1953.

[20] L. H. W, L. J. X and C. M. L, *Shell Theory*: Zhejiang University Press
, 1987.

[21] M. J. Guers, C. J. Fontana and B. R. Tittmann, "a Noninvasive Pressure Measurement Technique and the Potential for Integrated Calibration," in *REVIEW OF PROGRESS IN QUANTITATIVE NONDESTRUCTIVE EVALUATION: 34th Annual Review of Progress in Quantitative Nondestructive Evaluation*, 2008, pp. 1500-1504.

[22] N. R. Draper and H. Smith, *Applied regression analysis*: John Wiley & Sons, 2014.